National Institute for Aviation Research
Wichita State University
1845 Fairmount Box 93
Wichita, Kansas 67260-0093
(316) 978-8205
Melinda.laubach@wichita.edu

August 31, 2009

Mr. Marvin Nuss, Dr. Abali Abali, and Mr. Keith Noles

Attached is the final report for the failure analysis conducted on the Piper Comanche Horns (N7545P: PA 24-250, S/N 24-2752 and N5274P: PA 24-250, S/N 24-313). This analysis was performed at the request of the FAA with Mr. Nuss as the sponsor and Dr. Abali as the research program manager. Please direct any questions or comments regarding the contents of the report to me.

Regards,

Melinda Laubach
NIAR – Aging Aircraft Lab
Senior Research Engineer/Program Manager

M E M O R A N D U M

Date: 31 August 2009

To: Marvin Nuss, FAA Small Airplanes Directorate
Dr. Abali Abali, FAA, Technical Center
Keith Noles, Atlanta ACO Airframe Engineer for Piper products

From: Melinda Laubach, NIAR/ASTEC Aging Aircraft Laboratory

Re: **Metallurgical Evaluation of Two Piper Stabilator Horn Assemblies (**N7545P: PA 24-250, S/N 24-2752 and N5274P: PA 24-250, S/N 24-313**)**

Terms and Acronyms

- *Laboratory Fracture* – Area to which metallurgist applied stress on the specimen in order to break open the crack for visual inspection.
- *Woody Intergranular* – Surface giving the impression of being similar to wood fragments
- *Mud Cracking* – Surface giving the impression of being similar to dried out mud

NIAR –	National Institute for Aviation Research
FAA –	Federal Aviation Administration
ASTEC –	Aircraft Structural Testing and Evaluation Center
A/C –	Aircraft
FPI –	Fluorescent Penetrant Inspection
CVI –	Close Visual Inspection
S/N –	Serial Number
SB –	Small Bore Hole
LB –	Large Bore Hole
SCC –	Stress Corrosion Cracking

List of Figures

List of Tables

Background

The FAA submitted two Piper stabilator horn assembly forgings to NIAR with a request for failure analysis. The purpose of the analysis was to determine the root cause of in-service cracking in the subject parts. The two submitted parts were identified as follows:

1. Removed from 1961 PA 24-250, registry N7545P, S/N 24-2752 when the aircraft had 3,904 hours total time.
2. Removed from 1958 PA 24-250, registry N5274P, S/N 24-313 when the aircraft had approximately 4,000 hours total time.

Procedure

The two submitted parts were visually examined and photographed to show the as-received part condition pictured in Figure 1 through Figure 8. NIAR examiners did not visually find any lot markings, manufacturing logos, etc on the exterior or interior of the parts. Preexisting exterior damage/surface scratches prior to part disassembly are shown in Figure 2 and Figure 3. The diameters of the fastener holes and the large bores in the two parts were measured and compared to engineering drawings. The two parts were then subjected to a fluorescent penetrant inspection to determine the location and approximate extents of the cracking. Figure 9 to Figure 17 show the cracks prior to cutting the horn assemblies. These figures also identify the naming process for surfaces; Surface A interior LB hole surface (Figure 4 and Figure 8), Surface B interior SB hole surface (Figure 3 and Figure 7), and Surface C is the exterior location (Figure 3 and Figure 7). Figure 18 and Figure 19 show the fluorescent penetrant inspection (FPI) results for Hole 2 (A/C N7545P). This suspected crack location was determined to be only a surface scratch.

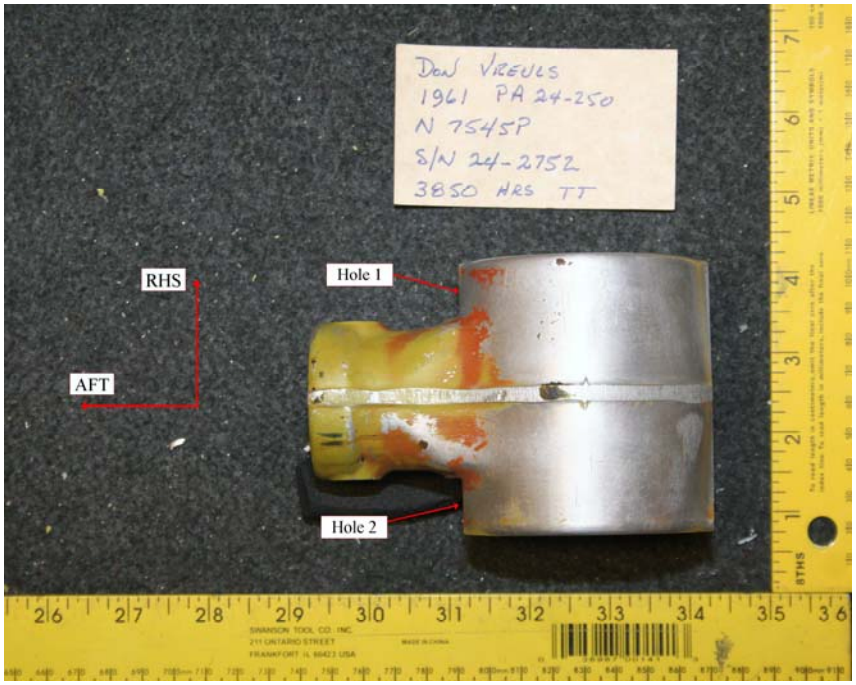

Figure 1 – Overview from A/C N7545P, Looking DWN

Figure 2 – Overview from A/C N7545P, Looking AFT

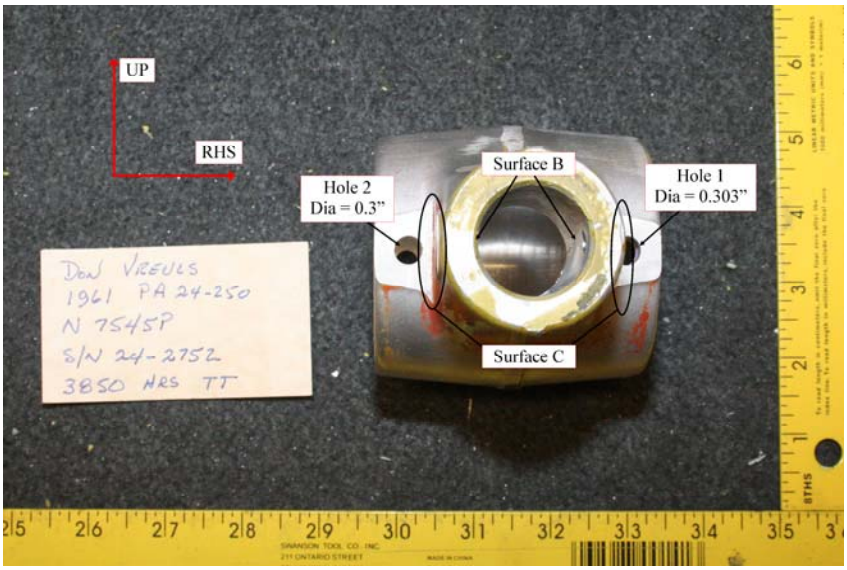

Figure 3 – Overview from A/C N7545P, Looking FWD

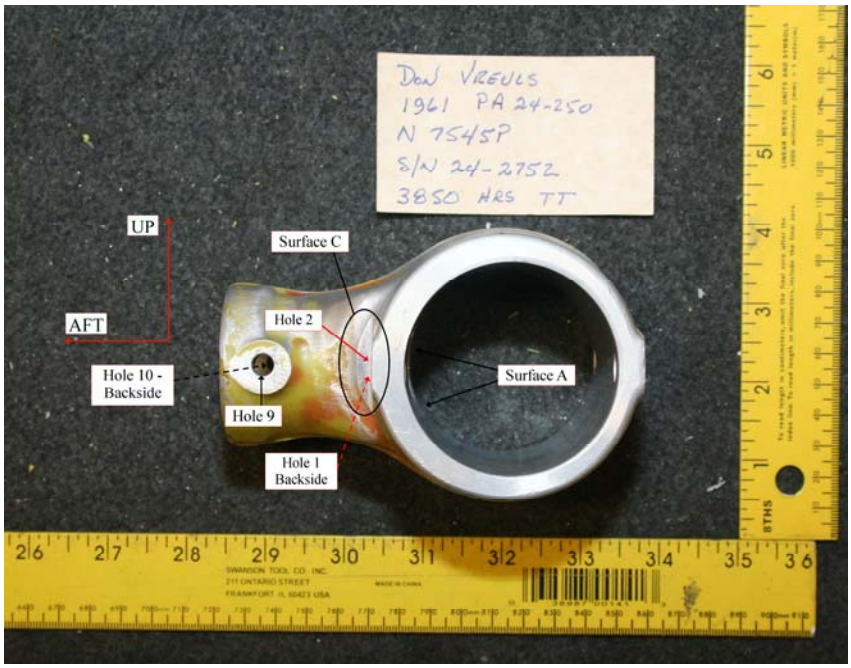

Figure 4 – Overview from A/C N7545P, Looking from the Side

Figure 5 – Overview from A/C N5274P, Looking DWN

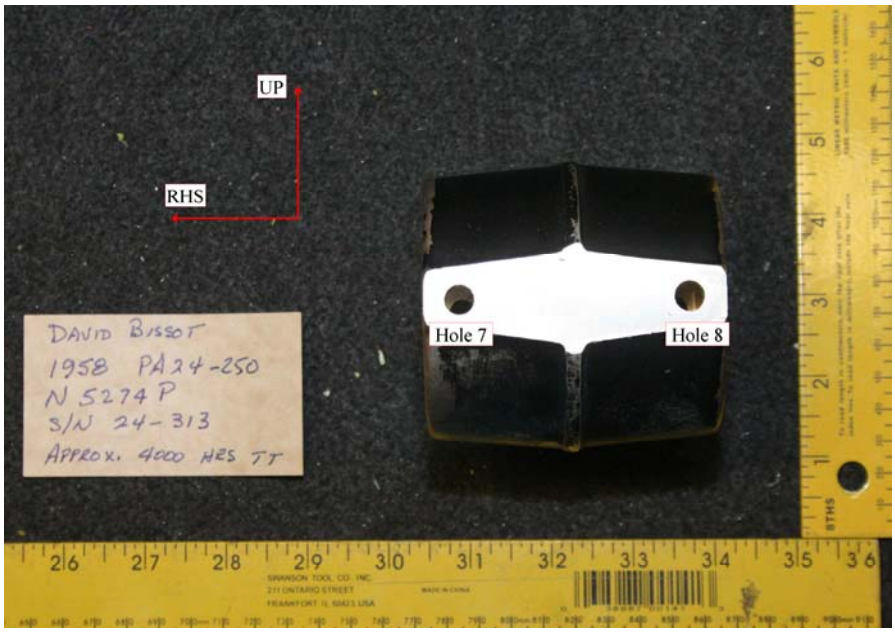

Figure 6 – Overview from A/C N5274P, Looking AFT

Figure 7 – Overview from A/C N5274P, Looking FWD

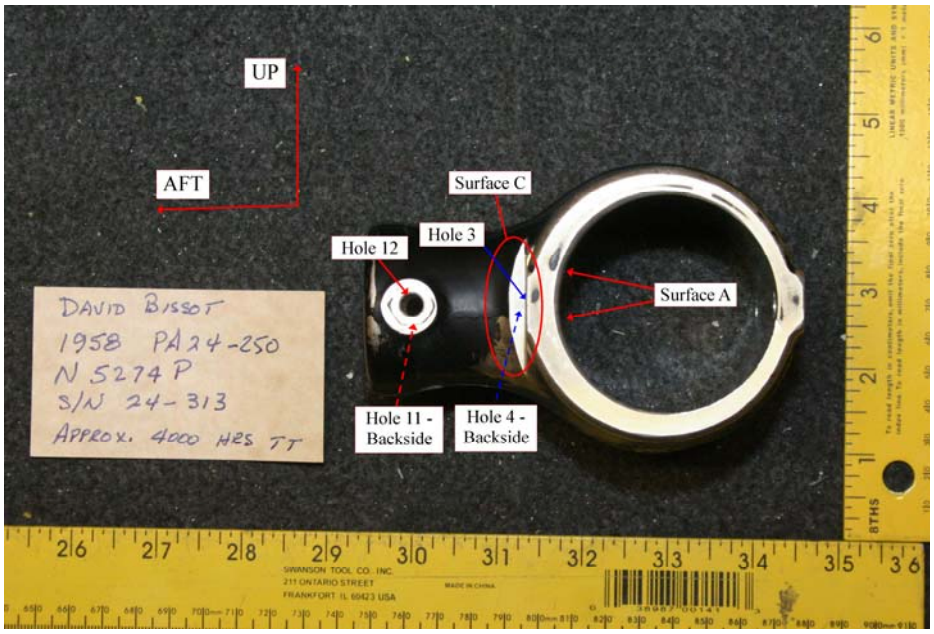

Figure 8 – Overview from A/C N5274P, Looking from the Side

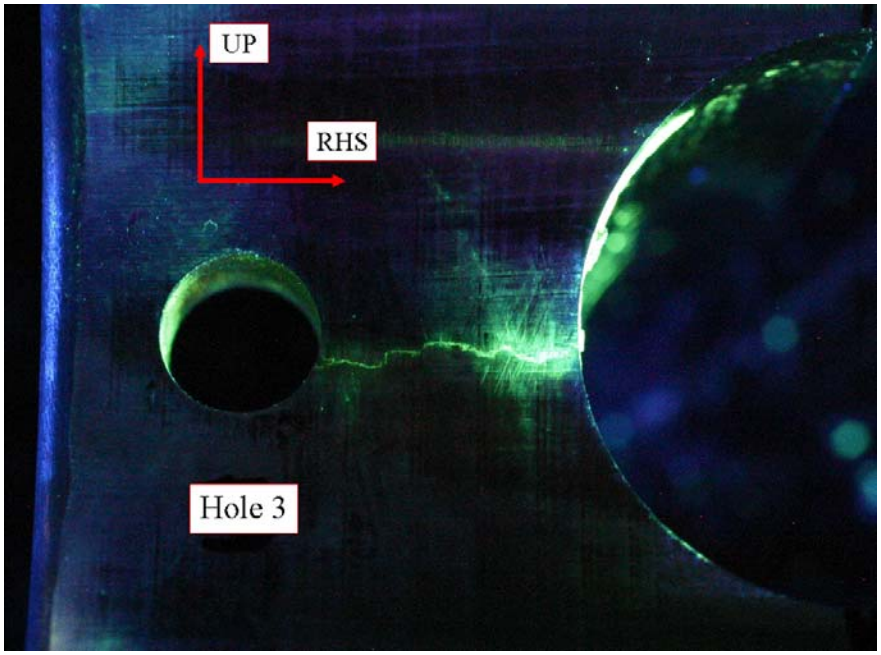

Figure 9 – FPI Hole 3 Crack, Surface A (A/C N5274P)

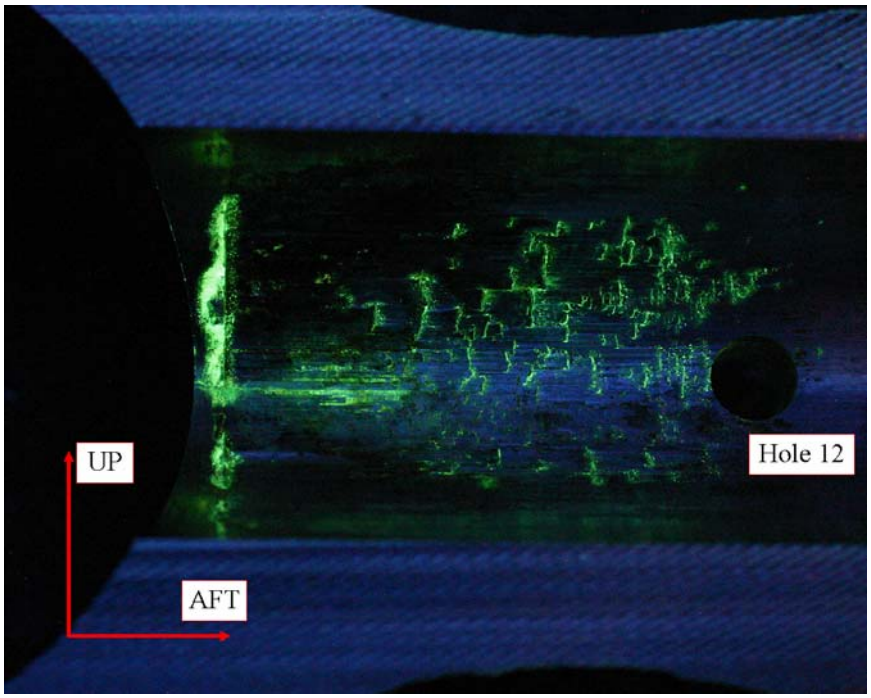

Figure 10 – FPI Hole 3 Crack, Surface B (A/C N5274P)

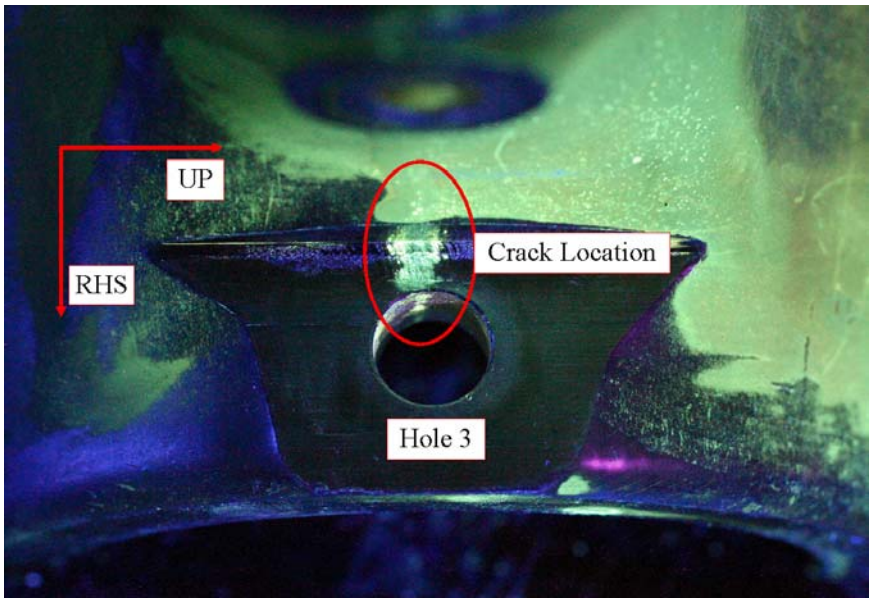

Figure 11 – FPI Hole 3 Crack, Surface C (A/C N5274P)

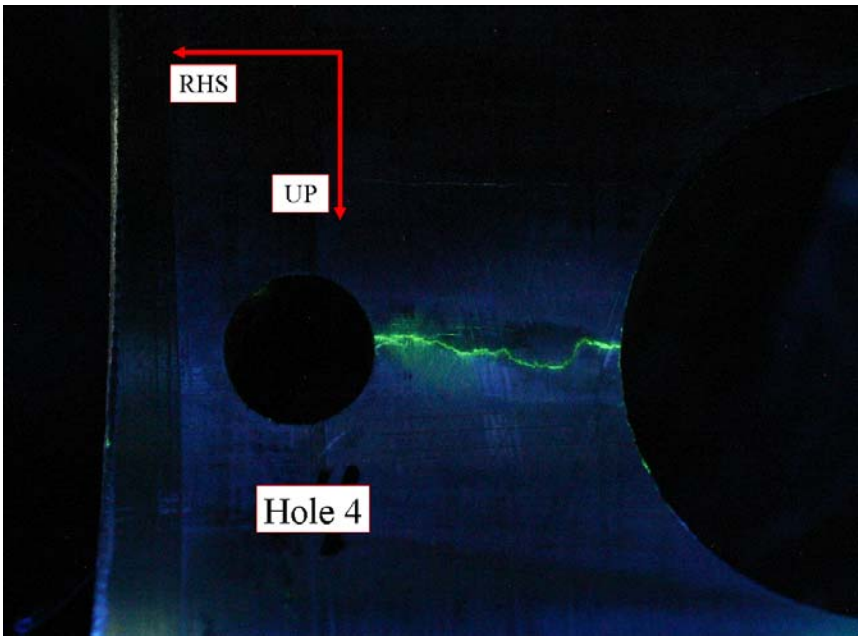

Figure 12 – FPI Hole 4 Crack, Surface A (A/C N5274P)

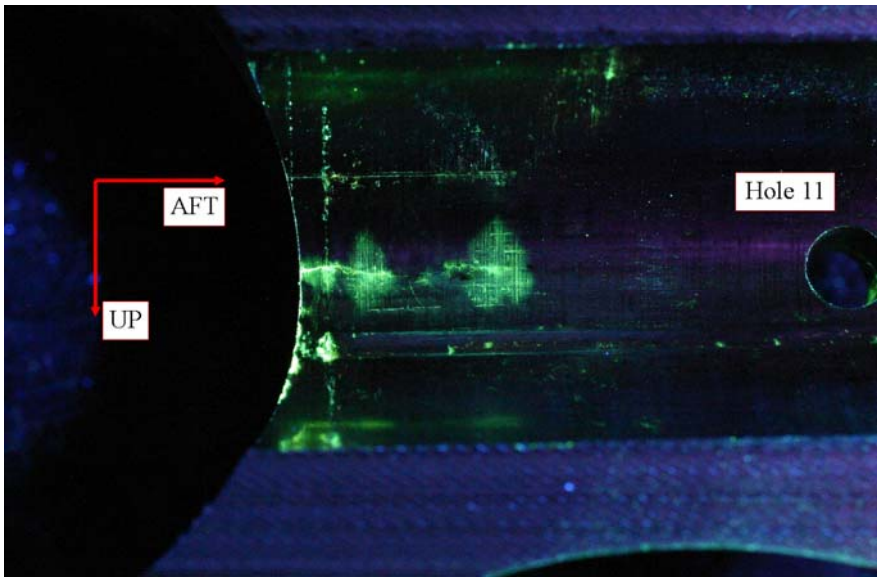

Figure 13 – FPI Hole 4 Crack, Surface B (A/C N5274P)

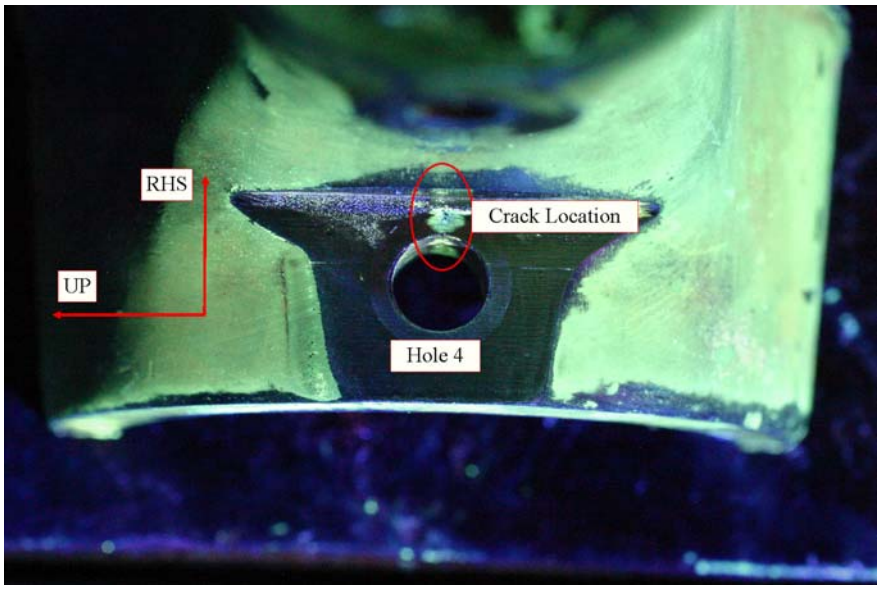

Figure 14 – FPI Hole 4 Crack, Surface C (A/C N5274P)

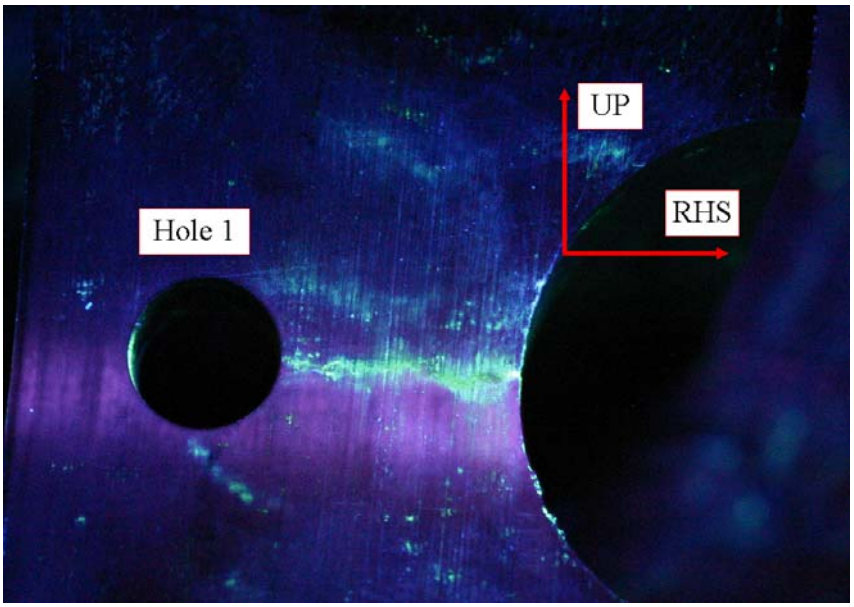

Figure 15 – FPI Hole 1 Crack, Surface A (A/C N7545P)

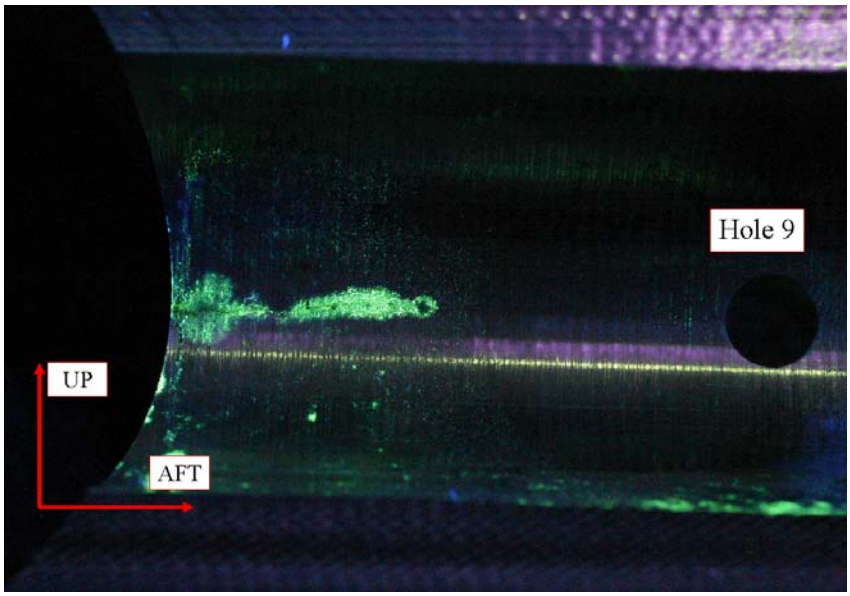

Figure 16 – FPI Hole 1 Crack, Surface B (A/C N7545P)

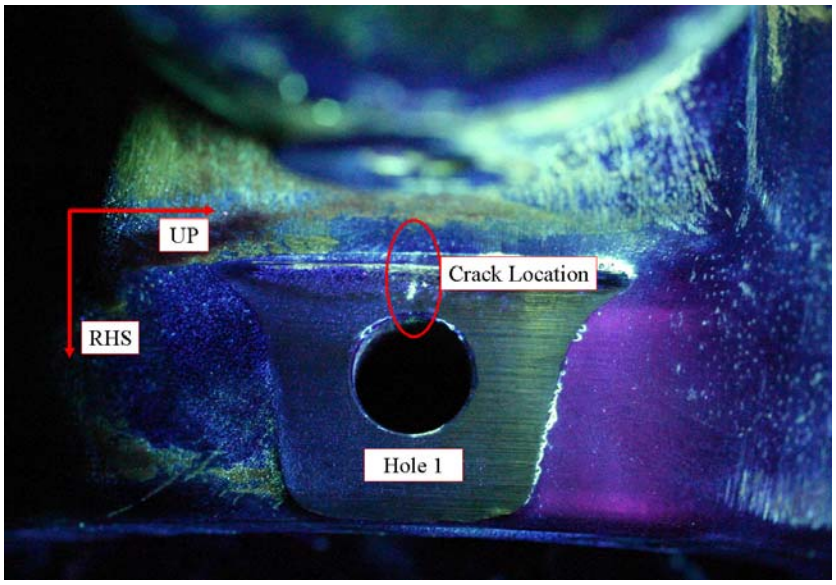

Figure 17 – FPI Hole 1 Crack, Surface C (A/C N7545P)

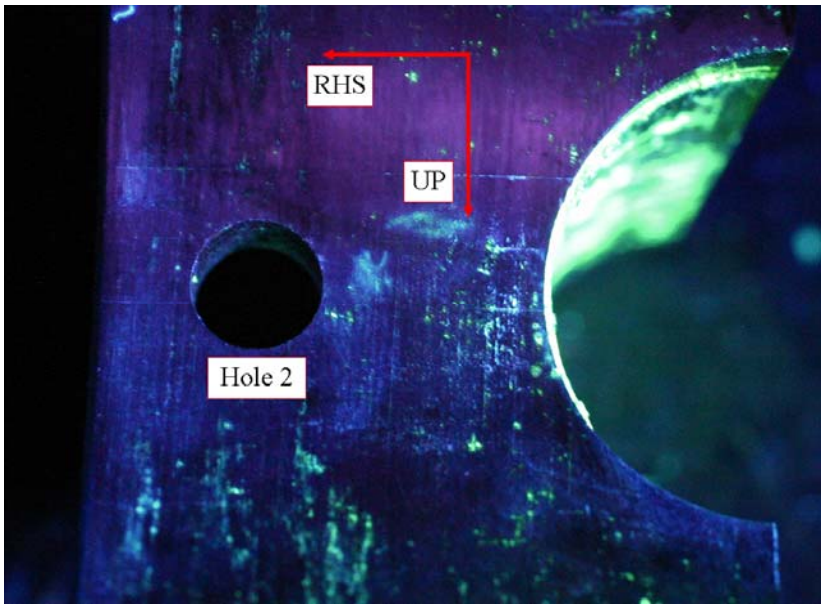

Figure 18 – FPI Hole 2, Surface A (A/C N7545P)

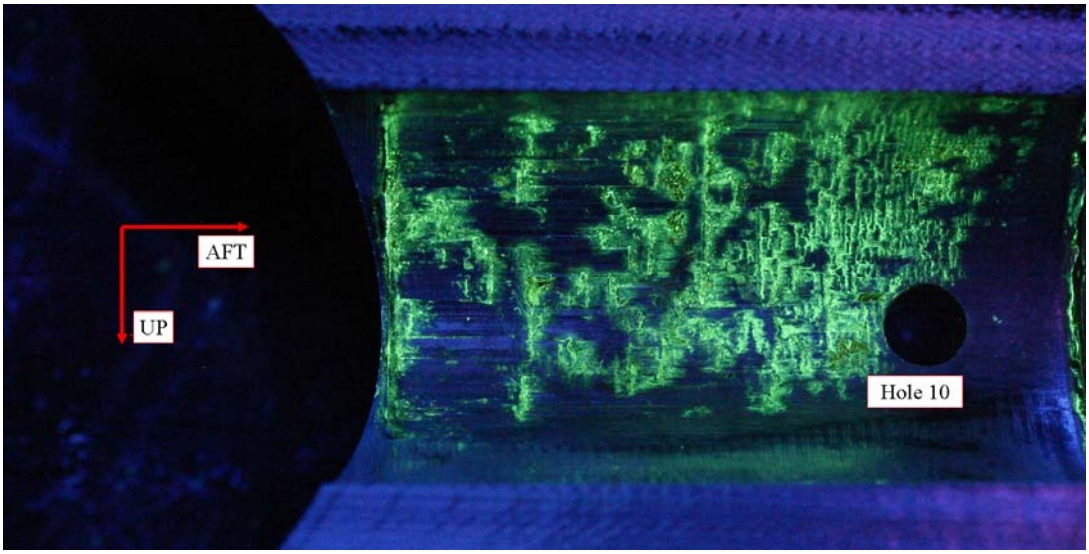

Figure 19 – FPI Hole 2, Surface B (A/C N7545P)

The parts were sectioned to obtain views of the interior surfaces near the cracks. Additional photographs were taken to show crack extents and the surface conditions adjacent to the cracks. Further cuts were made to open the cracks.

The crack faces were examined with low power optical microscopes and photographs were taken to show general crack face features. The crack faces were solvent cleaned to remove penetrant residues and other loose material. The crack faces were examined at higher magnification with optical microscopes and the scanning electron microscope. Electron fractographs were taken to show the typical crack face features and identify approximate crack origin locations.

A metallographic cross section was taken in the region where cracking occurred in a plane parallel to the plane of cracking. The cross section was mounted, polished, etched and microscopically

examined to view the grain flow characteristics and the typical material microstructure, photomicrographs where taken as required.

The chemical compositions of the two cracked parts were determined and compared to the required composition for 2014 aluminum forgings. Electrical conductivity and hardness measurements were made to verify that the two parts had been heat treated to the specified –T6 range.

Results

The submitted stabilator horn fitting identified as A/C N7545P is shown in Figure 4. The view is looking into the large 2.312 inch diameter bore of the part. A 0.25 inch diameter hole parallel to the large diameter bore is also visible in Figure 4.

A second view of the same part is shown in Figure 3. The view is looking into the smaller 1.118 inch diameter bore in the fitting. The two 0.30 inch diameter fastener holes parallel to the small diameter bore are visible in Figure 3.

In the stabilator horn assembly a steel tube is press fit into the 1.118 inch diameter bore and held in place by a fastener through the tube and the 0.25 inch hole identified in Figure 4. The exterior paint on the part in Figure 4 and Figure 3 has mostly worn away but there were traces of green primer and remnants of orange paint.

The second stabilator horn fitting (A/C N5274P) submitted is shown in Figure 7 and Figure 8. The views correspond to the similar views of the first part in Figure 3 and Figure 4. This part was painted black and the paint was still present on most of the exterior surfaces.

Measurements of the diameters of the fastener holes and the two bores on the horn fittings are shown in Table 1 and Table 2. Hole measurements found in Table 1 are approximate due to measurement procedure, age, and surface damage buildup. Similarly, the surfaces of the SB holes on both parts exhibited evidence of smeared metal and galling over relatively large areas which made made it difficult to precisely measure the diameters in Table 2. Examples of areas with smeared metal are shown in Figure 20 and Figure 21. The area in Figure 20 is located on Surface B presented in Figure 3. The area in Figure 21 is located on Surface B presented in Figure 7.

Hole Number	Inner Diameters (in)	Drawing Diameter Dimension (in)
1	0.3	0.301 - 0.304
2	0.3	0.301 - 0.304
3	0.3	0.301 - 0.304
4	0.3	0.301 - 0.304
5	0.3	0.301 - 0.304
6	0.3	0.301 - 0.304
7	0.3	0.301 - 0.304
8	0.3	0.301 - 0.304
9	0.25	0.249 - 0.251
10	0.25	0.249 - 0.251
11	0.25	0.249 - 0.251
12	0.25	0.249 - 0.251

Table 1 – Fastener Hole Diameter Measurements

	N754SP	N5274P	Drawing Diameter Dimension (in)
Small Bore Hole (in)	1.1	1.1	1.1185
Large Bore Hole (in)	2.3	2.3	2.312

Table 2 – LB and SB Hole Diameter Measurements

Figure 20 – Smeared Metal on Surface B from A/C N7545P

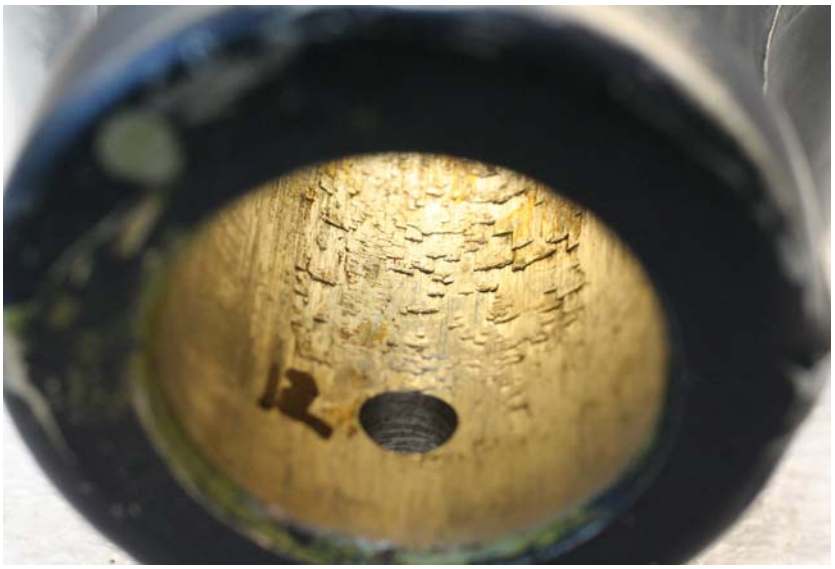

Figure 21 – Smeared Metal on Surface B from A/C N5274P

FPI of the two parts showed crack indications primarily on the interior surfaces of the two bores in the parts shown in Figure 9 through Figure 19. On the LB the crack indication was between the SB

and the 0.30 inch diameter fastener holes. The LB surfaces where crack indications were observed are shown in Figure 22 and Figure 23. Areas of interest are identified by Hole numbers 1 and 2 in Figure 22 and Hole numbers 3 and 4 in Figure 23.

Figure 22 – Surface A of the Large Diameter Bore from A/C N7545P

Figure 23 – Surface A of the Large Diameter Bore from A/C N5274P

Penetrant indications and visual cracks were observed in areas 1, 3 and 4 extending from the 1.118 inch diameter hole to the corresponding 0.30 inch diameter hole. No cracking was identified in or around Hole 2 on the part A/C N7545P by either visual or fluorescent penetrant inspection.

The three cracks observed (1 crack in N7545P and 2 cracks in N5274P) were also detected on the surface of the 1.118 inch diameter bore visually and with penetrant. The galling and smeared metal on the SB surfaces made it difficult to determine exact crack length either visually, with penetrant, or eddy current surface scanning. An example is shown in Figure 24. The cracking on Surface B, on A/C N5274P is visible at the intersection of the two larger bores but is difficult to detect on the rough surface of the smaller bore. There were also signs of rusting throughout the SB hole, due to the steel tube inserted during production.

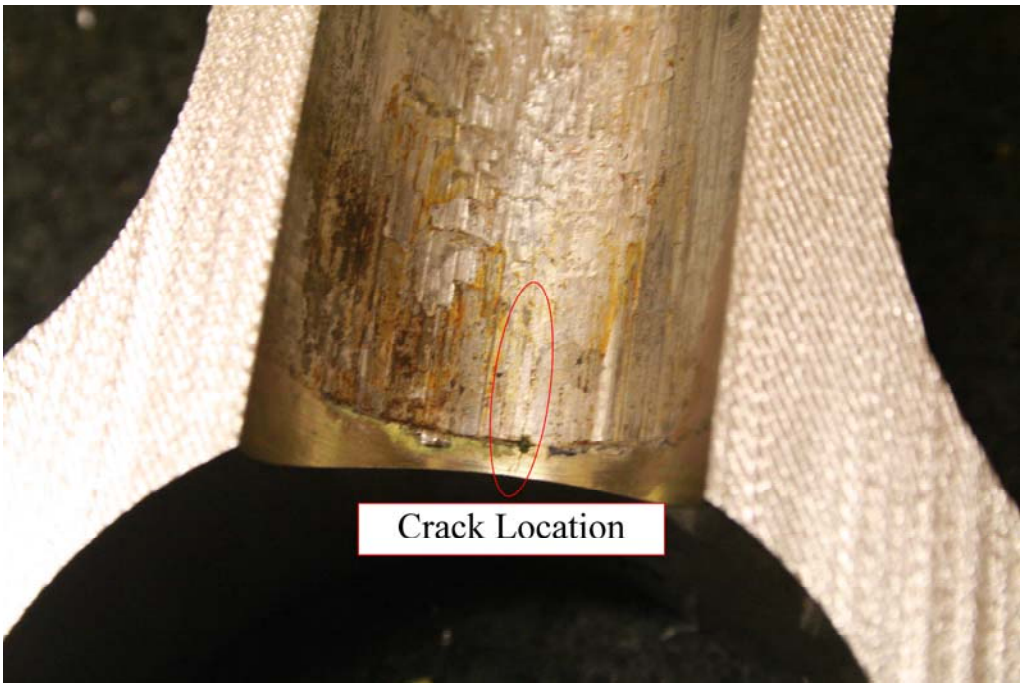

Figure 24 – Cracking and Roughness on Surface B from A/C N5274P

The three cracks all appeared to be at least 0.5 inch long on the small bore surface. All of the three cracks found were observed visually and with penetrant inspection on the part exterior surface at the edge of the 0.30 inch diameter fastener holes. A typical example (Hole 1 Crack from A/C N7545P) is shown in Figure 25.

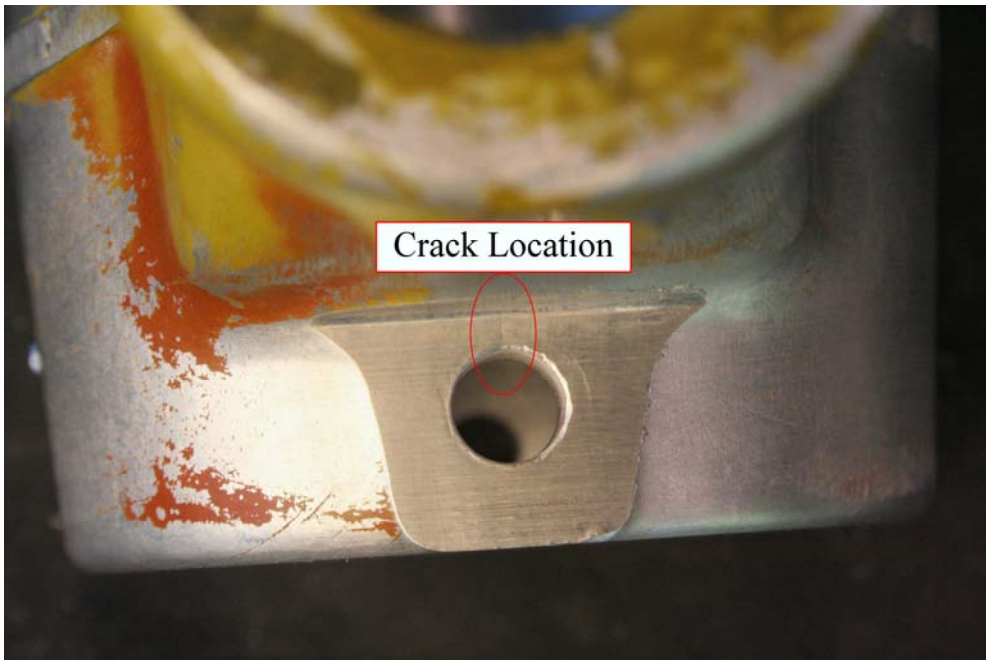

Figure 25 – Hole 1 Crack Penetrating on Surface C, A/C N5274P

Examination of the faces of the opened cracks showed general features typical of stress corrosion cracking. The faces had a "woody" intergranular appearance and there was evidence of corrosion products on the faces. The face of the crack in Hole 1 from A/C N7545P is shown in Figure 26. The face was covered with corrosion products and had a reddish tint which may have been remnants from a previous dye penetrant inspection. Solvent cleaning of the face removed the reddish color but much of the other material remained on the face. The dimensions of the cracking along the two bore surfaces are indicated in Figure 26.

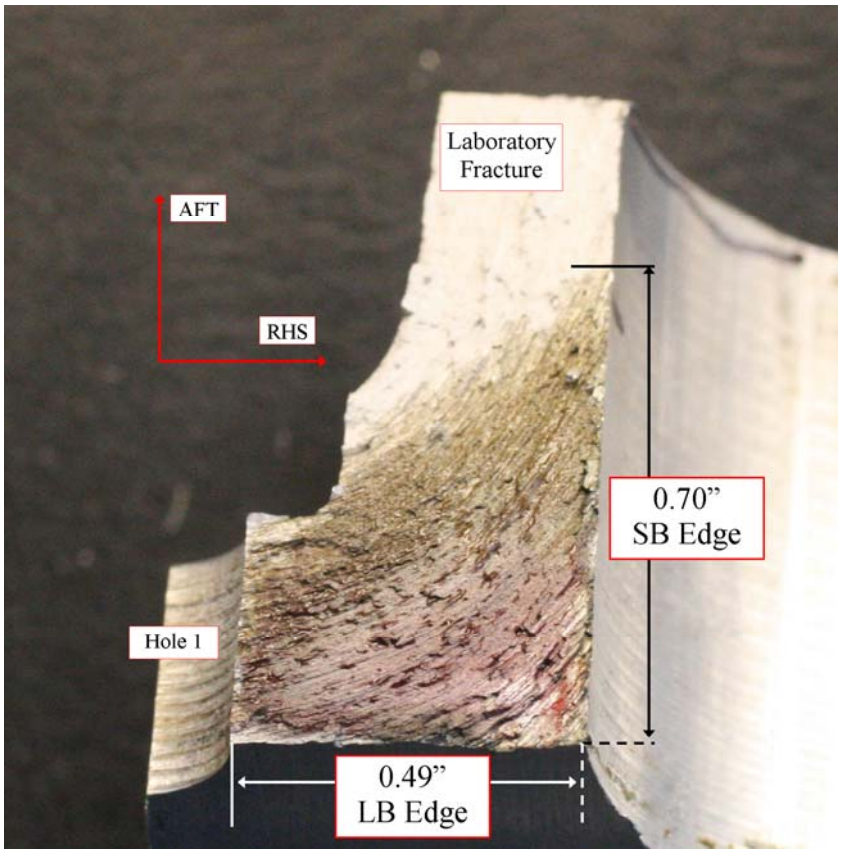

Figure 26 – Face of Hole 1 Crack from A/C N7545P

The face of the crack detected in Hole 3 of the part from A/C N5274P is shown in Figure 27. The green color on the face is fluorescent penetrant remnants which were removed with solvent cleaning. The SB surface exhibited rough areas with a rust color. There also were local areas on the crack face along the edge of the SB with a rust color. Maximum dimensions of cracking along the two bores are indicated.

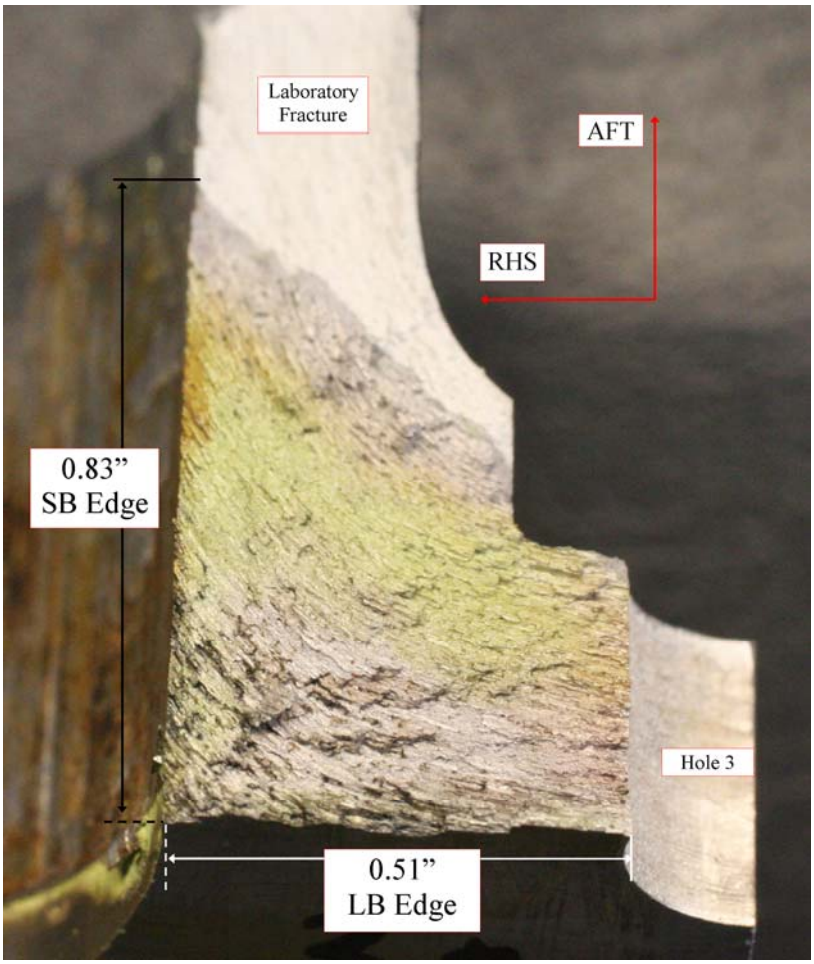

Figure 27 – Face of Hole 3 Crack from A/C N5274P

The face of the crack detected in Hole 4 of the part from A/C N5274P is shown in Figure 28. The face has been solvent cleaned, but there are still areas with a rust color along the edge of the SB hole.

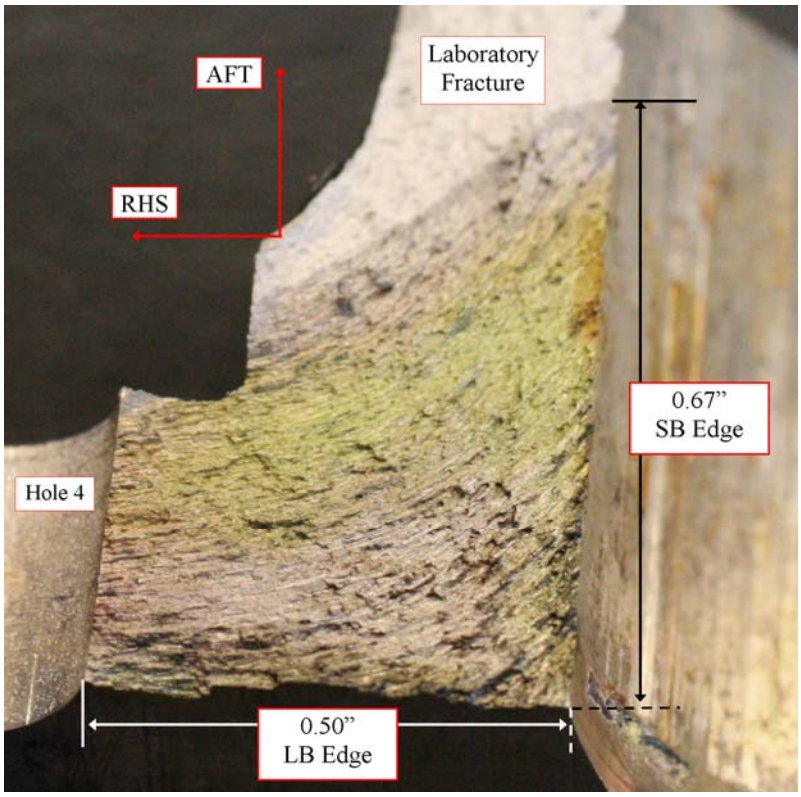

Figure 28 – Face of Hole 4 Crack from A/C N5274P

The exact origins of cracking could not be readily identified on the faces of the three cracks. Stress corrosion cracking tends to have multiple origins in slightly different planes and propagate along grain boundaries following the grain flow. All three of the cracks had evidence of flow across the corner of the face at the intersection of the two large bores.

Higher magnification examination of the crack faces confirmed that cracking was due to stress corrosion. The cracking was intergranular and followed the grain flow of the part. There was evidence of corrosion scale that had not been removed by cleaning the crack faces. On each of the crack faces there was pronounced grain flow across the corner formed by the intersection of the two bores. The features at the corner of the faces of the crack are shown in Figure 29.

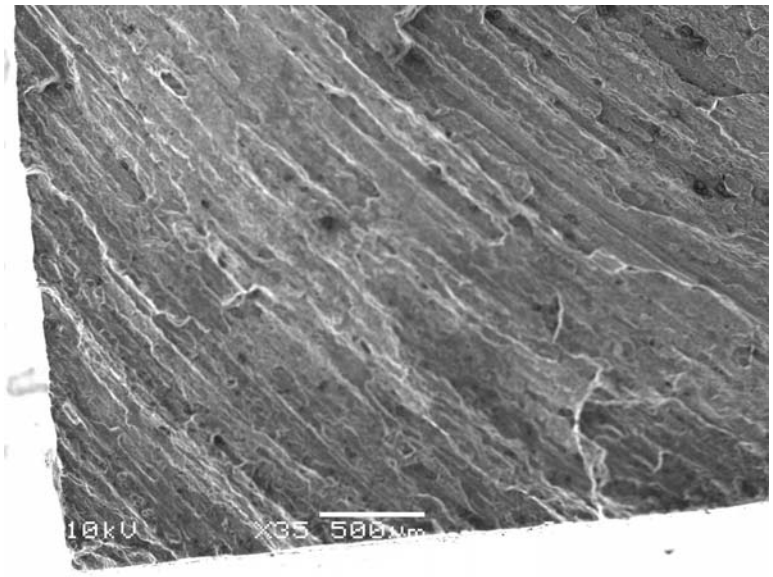

Figure 29 – Corner of Crack Face from A/C N7545P

The corresponding features at the corner of the crack face at Hole 3 of A/C N5274P are shown in Figure 30.

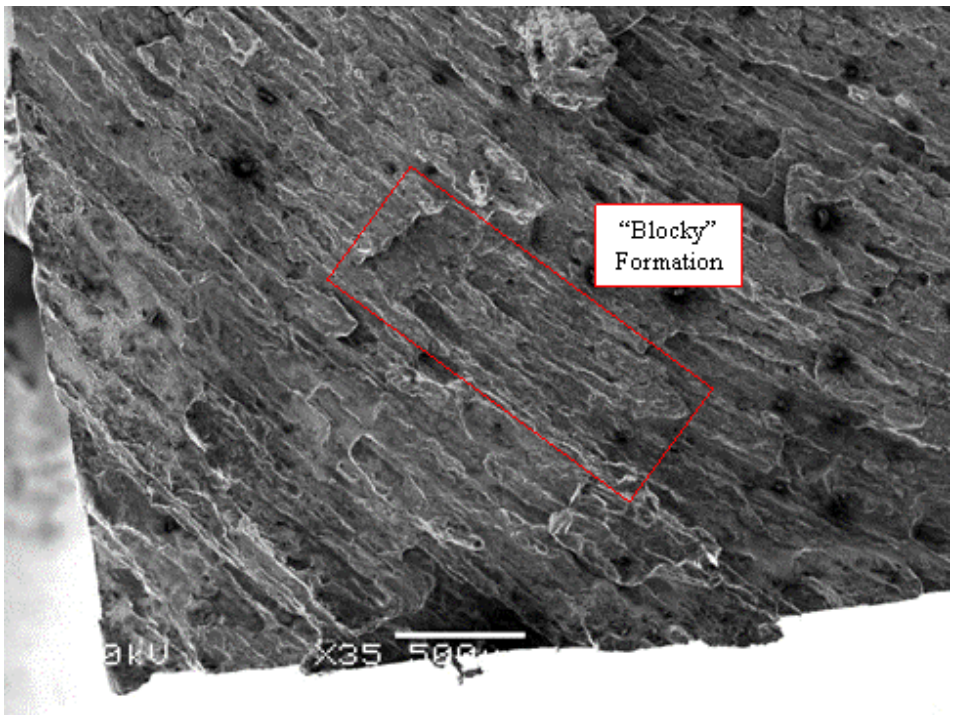

Figure 30 – Corner of the Crack Face, Hole 3 from A/C N5274P

The grain flow characteristics in the two figures showed that the machining of the two bores had caused an end grain condition to be at least partially exposed to both machined surfaces near the intersection. Since the grain flow runs approximately at a 45 degree angle in Figure 30 due to the forging

process and galling exists in the SB hole, the exposed grain boundries provided nucleation orgins for SCC. This partially adverse grain flow condition was a factor in the cracking. Hole 2 had the same evidence of grain flow and galling as shown in Figure 19, but did not show any evidence of cracking.

An electron fractograph of typical crack faces features at higher magnification is shown in Figure 31. A "blocky" looking region had intergranular features and some evidence of corrosion products on the surfaces shown in the fractograph. The area shown was located a short distance from the corner of the face of the crack, part A/C N7545P.

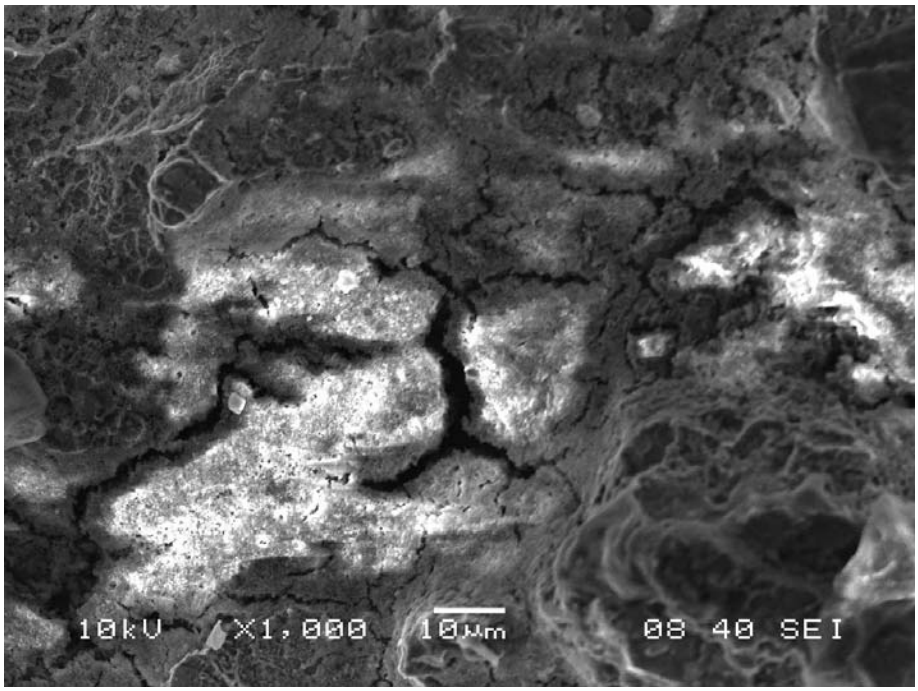

Figure 31 – Electron Fractograph of Intergranular Crack Face from A/C N7545P

Another area with the stress corrosion cracking features is shown in Figure 32. There is a general block looking intergranular appearance with evidence of a heavy corrosion scale. There is an appearance of "mud cracking" in the scaled areas where there is a characteristic of stress corrosion cracking. The area shown was located a short distance from the corner of Hole 3 crack face shown in Figure 27.

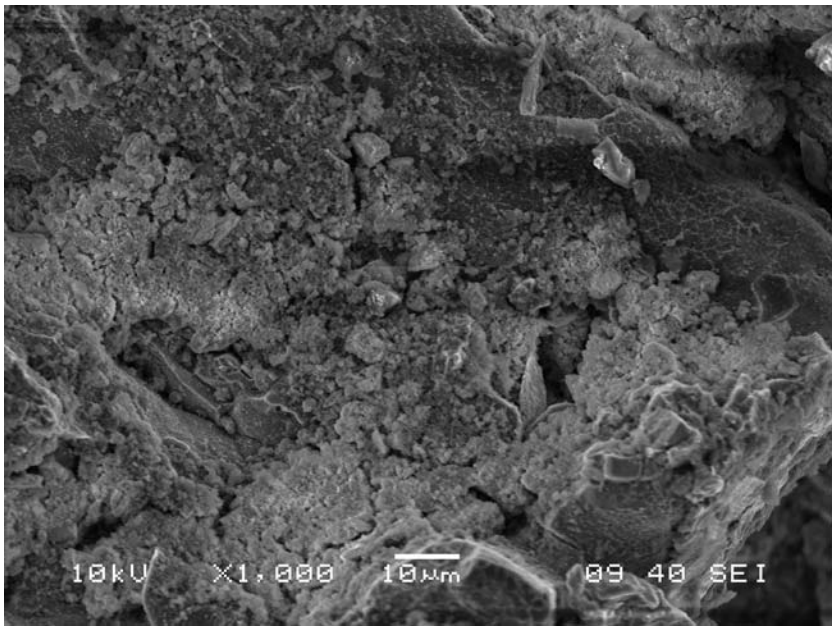

Figure 32 – Intergranular Features with a Corrosion Scale from A/C N5274P

The examination of the crack face with the scanning electron microscope did not identify any evidence of crack growth due to fatigue.

The metallographic cross section was taken in the area identified as Hole 2 in Figure 22. The cross section was in the same plane as the plane of cracking at the other three locations. The overall grain flow in this region corresponded well to the "flow" observed on the crack faces. The overall grain flow is shown in Figure 33. The observed pattern confirmed that there was at least partial exposure to an end grain condition on both bore surfaces near the corner.

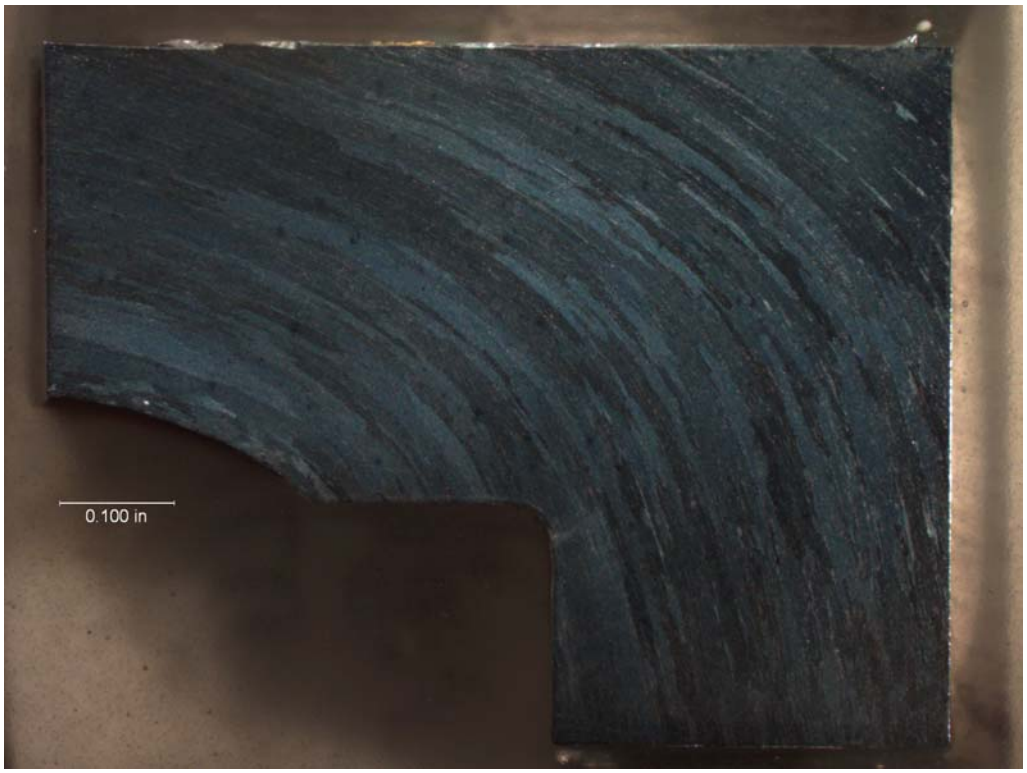

Figure 33 – Grain Flow Pattern from A/C N7545P

The rough surface along the small diameter bore is visible at the top in Figure 33. The grain size in Figure 33 appears to be relatively large but part of that may be due to the short transverse grain direction being perpendicular to the plane of observation. Figure 33 shows grain flow near hole 2, the non-cracked location. Figure 26 through Figure 28 show the same grain flow characteristics as expressed in Figure 33.

The typical material microstructure on the cross section is shown in Figure 34. The area shown was a short distance from the intersection of the two bores in the part. The microstructure was typical for 2014 aluminum forgings.

Figure 34 – Typical Material Microstructure

The chemical compositions of the two submitted parts met the requirements for 2014 aluminum forgings as shown in Table 3.

Element	Composition Percent (%)		
	A/C N5274P	A/C N7545P	Required QQ-A-36
Manganese	0.82	0.65	0.40 - 1.20
Silicon	0.91	0.93	0.50 - 1.20
Copper	4.6	4.5	3.9 - 5.0
Chromium	0.02	0.04	0.1 Max
Manganese	0.55	0.72	0.20 - 0.90
Zinc	0.24	0.2	0.25 Max
Iron	0.48	0.44	0.7 Max
Titanium	0.04	0.04	0.15 Max
Aluminum	Base	Base	Remainder

Table 3 – Typical Material Microstructure

The hardness and electrical conductivity of the two parts were within normal ranges for 2014 aluminum forgings heat treated to the –T6 condition. Values for Hardnesss and Electrical Conductivity are expressed in Table 4.

	N5274P	N7545P	Reference Material
Hardness (HRBW)	85	85	78 - 89
Electrical Conductivity (S m^{-1})	37	37	35 - 40

Table 4 – Hardness and Electrical Conductivity